Energy Storage Materials 13 (2018) 241–246

Contents lists available at ScienceDirect

Energy Storage Materials

journal homepage: www.elsevier.com/locate/ensm

Quantitative investigation of polysulfide adsorption capability of candidate materials for Li-S batteries

David Sichen Wu[a], Feifei Shi[a], Guangmin Zhou[a], Chenxi Zu[a], Chong Liu[a], Kai Liu[a], Yayuan Liu[a], Jiangyan Wang[a], Yucan Peng[a], Yi Cui[a,b,*]

[a] Department of Materials Science and Engineering, Stanford University, Stanford, CA 94305, USA
[b] Stanford Institute for Materials and Energy Sciences, SLAC National Accelerator Laboratory, 2575 Sand Hill Road, Menlo Park, CA 94025, USA

ARTICLE INFO

Keywords:
Lithium sulfur batteries
polysulfide adsorption

ABSTRACT

Lithium-sulfur batteries have a high theoretical energy density of 2500 Wh/kg and are promising candidates for meeting future energy storage demands. However, dissolution of the intermediate polysulfide species into the electrolyte remains as a major challenge, causing fast capacity degradation in Li-S batteries. Many recent studies have reported various materials such as metal oxides and sulfides that interact strongly with polysulfide species and can alleviate the dissolution problem, though little work has focused on quantitative comparison of different materials under equivalent conditions. Here, we establish a standard procedure to quantitatively compare the polysulfide adsorption capability of candidate materials. We found that an order of magnitude of difference is evident between poor adsorption materials such as carbon black and strong adsorption materials such as V_2O_5 and MnO_2. We elucidate different adsorption mechanisms may be present and probe possible adsorption species. We expect our work will provide a useful strategy to screen for suitable candidate materials and valuable information for rational design of long cycle life Li-S batteries.

1. Introduction

Next generation energy storage systems are needed to satisfy the emerging electric vehicles and renewable energy storage markets. Rechargeable lithium-sulfur batteries are very promising candidates because of their high theoretical energy density compared to conventional lithium-ion batteries (~ 2500 Wh/kg vs. ~ 420 Wh/kg) [1–3]. Furthermore, sulfur is cheap and abundant, making it attractive for a low-cost system. Ongoing research has presented ways to tackle the volumetric expansion (~ 80%) of sulfur upon lithiation to lithium sulfide, and ameliorate the low conductivity of sulfur and lithium sulfide [4–10]. However, fast capacity degradation of lithium-sulfur batteries remains as a major problem. This is because the long-chain lithium polysulfides, which are intermediates of the redox reaction from sulfur to lithium sulfide, are soluble in the organic electrolyte. This dissolution leads to parasitic reactions, incomplete sulfur utilization and low coulombic efficiency for the lithium-sulfur batteries [11–14].

Early strategies to address this problem involved physically confining the soluble polysulfides via hosts with high surface area and/or suitable pore structures, such as mesoporous/microporous carbon and porous hollow carbon spheres [15–17]. These showed great capacity improvements over the first few hundred cycles, but suffer significant decay thereafter due to the weak interaction between the polar polysulfides and non-polar carbon host. Inevitably the polysulfides leak out and physical trapping becomes ineffective. Materials that bind polysulfides through chemical interactions are much more promising and many metal oxides such as Al_2O_3, SiO_2, TiO_2, Ti_4O_7 and MnO_2 have been reported in literature to significantly improve long term cycling performance [18–25]. More recently, metal sulfides and metal nitrides have also been reported to greatly enhance cycling performance [26–28]. With a plethora of additives and hosts available, it is crucial to establish a standard procedure to quantitatively compare their polysulfide adsorption capability. This information can be invaluable in the design of lithium-sulfur batteries to determine suitable candidate materials and the appropriate amount of surface area required.

Here, we establish a possible protocol to quantitatively compare the polysulfide adsorption capability of various materials. The methodology can be further applied to more extensive lists of additives and hosts. Based on interest and availability, seven metal oxides, seven metal sulfides and one metal nitride are selected as candidate materials to be reported here. It has been shown through theoretical calculations that oxygen, sulfur, and nitrogen functional groups can have strong

* Corresponding author at: Department of Materials Science and Engineering, Stanford University, Stanford, CA 94305, USA .
E-mail address: yicui@stanford.edu (Y. Cui).

https://doi.org/10.1016/j.ensm.2018.01.020
Received 2 October 2017; Received in revised form 26 January 2018; Accepted 31 January 2018
Available online 03 February 2018
2405-8297/

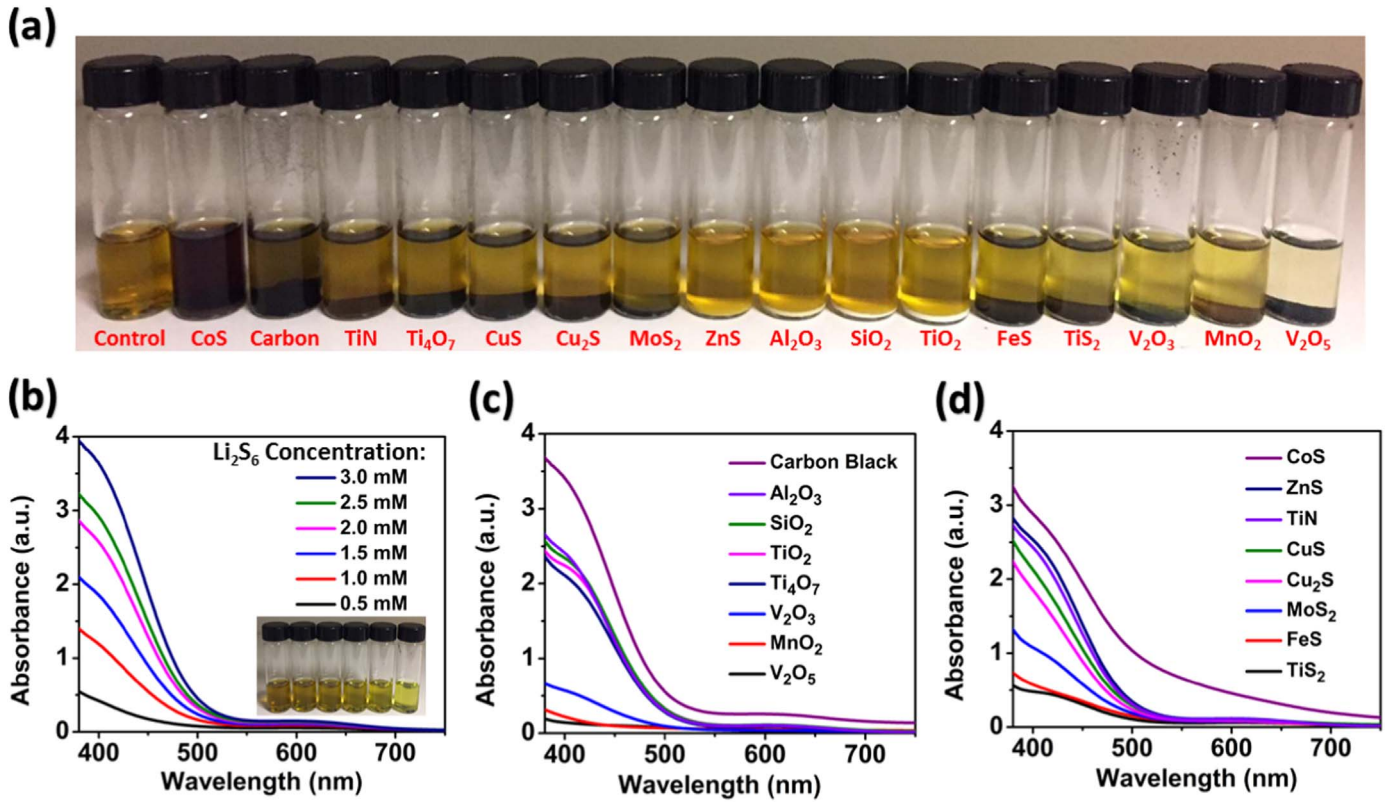

Fig. 1. Li_2S_6 polysulfide adsorption test: a) photograph of setup. b) UV-Vis data of varying concentrations of Li_2S_6 in DOL/DME solution without candidate materials, c-d) with candidate materials added in 3 mM Li_2S_6.

interactions with polysulfide species [29,30]. Carbon black, a common additive, is also selected for comparison. In order to normalize for surface area, Brunauer-Emmett-Teller theory analysis is performed on commercial powders of all 16 candidate materials (Supporting Fig. S1). The adsorption test setup is generic and the choice of polysulfide species, concentration, type and amount of electrolyte solution, surface area of candidate materials, exposure time and other parameters may be varied. We select one fixed set as the standard conditions to compare and discuss in detail. Fig. 1 presents data for the setup where 0.5 m^2 surface area of candidate materials are added to 3 mM of Li_2S_6 in 4 mL of 1,3-dioxolane/1,2-dimethoxyethane solution (DOL/DME, 1:1 by volume) for 3 hours. Li_2S_6 is a representative soluble long-chain polysulfide species and is prepared by chemically reacting sulfur with Li_2S in DOL/DME solution which is a common electrolyte system for Li-S batteries.

2. Materials and methods

2.1. BET analysis

About 200 mg of each candidate material was heated to 120 °C and degassed for 10 hours via the Micromeritics ASAP 2020 Surface Area and Porosity Analyzer. The BET specific surface area was tested by nitrogen adsorption-desorption measurement at −196 °C.

2.2. Adsorption of lithium polysulfide

All samples were dried under vacuum at 80 °C overnight before the adsorption test. Li_2S_6 was prepared by chemically reacting sublimed sulfur and an appropriate amount of Li_2S in DOL/DME solution (1:1 by volume). The solution was then stirred at 70 °C in an Ar-filled glove box overnight to produce a brownish-red Li_2S_6 solution (0.25 M). The Li_2S_6 was then diluted to 3 mM for the polysulfide adsorption test.

2.3. UV–vis spectroscopy

0.5 m^2 of each candidate material was placed in 4 mL of DOL/DME solution (1:1 by volume) in an Ar-filled glove box. 3 mM Li_2S_6 were introduced to all samples and allowed to rest for 3 hours. 2 mL of supernatant solutions were then extracted and sealed. UV–vis analysis was performed on the supernatant solutions via Agilent Cary 6000i UV/Vis/NIR instrument. To improve the reliability of data, 10 sets of repetitions were performed.

2.4. ICP-AES measurements

Known amounts of $CuSO_4.5H_2O$ and $LiNO_3$ were dissolved in 200 mL deionized water for calibrations of S and Li intensities in order to account for offsets potentially inherent in the methodology. Known concentrations (0.5 mM to 3.0 mM) of Li_2S_6 were diluted 200× times in 10 mL deionized water as control and calibration samples. Supernatant solutions from polysulfide adsorption test of candidate materials were also diluted 200× times in 10 mL deionized water and subjected to ICP-AES measurement for S and Li intensities. To improve the reliability of data, 21 sets of samples were prepared and tested for each of the 16 candidate materials and 7 control concentrations.

2.5. XPS analysis

Candidate materials post polysulfide adsorption test were subjected to centrifuge treatment for ease of separation. The supernatant Li_2S_6 solutions were poured away and the remaining candidate material powders were mounted and placed in a vacuum chamber. XPS analysis was performed on the material surface using a PHI Versaprobe 1 Scanning XPS Microprobe system with monochromatic Al (Kα) radiation (1486 eV). Carbon 1s peaks of samples were calibrated. Sulfur 2p peaks were examined in detail.

Table 1
Polysulfide adsorption capabilities of candidate materials and species observed on surfaces.

Candidate Material	UV–vis Li_2S_6 Adsorption[a] ($\mu mol/m^2$)	UV–vis Li_2S_6 Adsorption[a] (mg/m^2)	ICP-AES Li_2S_6 Adsorption ($\mu mol/m^2$)	ICP-AES Li_2S_6 Adsorption (mg/m^2)	Species Observed[b] via XPS
V_2O_5	23.1	4.8	22.3	4.6	PT, T
MnO_2	22.5	4.6	22.9	4.7	PT
TiS_2	20.8	4.3	21.4	4.4	PT, T, PS
V_2O_3	20.2	4.2	19.9	4.1	T
FeS	20.2	4.2	20.9	4.3	PT, PS
MoS_2	16.9	3.5	17.5	3.6	PS
Cu_2S	11.8	2.4	11.9	2.5	PT, PS
Ti_4O_7	10.1	2.1	10.1	2.1	PS
CuS	10.0	2.1	9.3	1.9	PS
TiO_2	9.2	1.9	9.0	1.9	PS
SiO_2	8.5	1.8	6.6	1.4	PS
Al_2O_3	8.1	1.7	6.1	1.3	PS
TiN	8.0	1.6	6.9	1.4	PS
ZnS	7.3	1.5	5.4	1.1	PS
CoS	2.6	0.5	3.5	0.7	PT, PS
Carbon Black	1.3	0.3	1.6	0.3	PS

[a] Calculated at 400 nm wavelength.
[b] PT = polythionate, T = thiosulfate, PS = polysulfide.

3. Results and discussion

As Fig. 1a illustrates, varying degrees of color change can be observed which are attributed to the interactions between candidate materials and the polysulfide species. No observable color fading is associated with carbon black, suggesting weak physical adsorption. Other materials such as MoS_2 and TiO_2 demonstrate higher adsorption capability compared to carbon black, while CoS and TiN exhibit relatively low adsorption capability as indicated by the lack of significant color fading. In contrast, the polysulfide solutions become much lighter in color after the addition of V_2O_5, MnO_2, V_2O_3, TiS_2 and FeS, suggesting strong interactions between Li_2S_6 and these materials. However, the judgment of color shades is subjective to the human eyes and is also hindered by the powder color of the candidate materials. Therefore, upon completion of the adsorption tests, 2 mL of the supernatant solutions are extracted from each sample to minimize the impact of powders and ultraviolet-visible spectroscopy (UV–vis) is performed on these supernatant solutions for detailed examination.

Fig. 1b illustrates the UV–vis performance in the visible spectrum of varying concentrations of Li_2S_6 without the addition of any candidate materials. There is strong absorbance towards the blue end of the visible spectrum, as blue is the complementary color of yellow. Unsurprisingly, higher concentrations of Li_2S_6 corresponds to darker shades of yellow and stronger absorbance around the blue spectrum. Fig. 1c shows the performance of carbon black and the metal oxides adsorption test supernatant solutions. The results are in good agreement with previous visual inspections. Carbon black demonstrates much higher blue spectrum absorbance corresponding to a higher concentration of Li_2S_6 remaining and thus weak polysulfide adsorption capability. In comparison to Fig. 1b, it can be seen that very little Li_2S_6 is adsorbed by carbon black with 3 mM being the original concentration in each adsorption test sample. In contrast, V_2O_5, MnO_2 and V_2O_3 all illustrate much higher adsorption capability showing very low concentrations of Li_2S_6 remaining in the supernatant solutions. Ti_4O_7, TiO_2, SiO_2 and Al_2O_3 exhibit moderate polysulfide adsorption capabilities. Similarly, Fig. 1d shows the performance of the metal nitride and metal sulfides. TiS_2, FeS and MoS_2 exhibit great polysulfide adsorption capabilities, CoS displays poor capability, while Cu_2S, CuS, TiN and ZnS exhibit moderate capabilities. In Fig. 1c and d, CoS and carbon black display background absorbance throughout the entire spectrum, this is likely due to the scattering effect of the sample powders, which do not settle well as evident in Fig. 1a and are present in the supernatant solutions.

To quantitatively approximate the polysulfide adsorption capabilities, the Beer-Lambert law can be employed: $A = \log_{10}(I_0/I) = L\varepsilon c$, where A is the absorbance of the sample, I_0 is the initial light intensity, I is the transmitted light intensity, L is the path length, ε is the molar absorptivity and c is the concentration. For our setup, the path length L is constant, the molar absorptivity ε is also constant for any particular wavelength, therefore the absorbance should vary directly with concentration c of polysulfide species in solution. Consequently, based on the remaining Li_2S_6 concentration in supernatant solution, it is possible to calculate the polysulfide adsorption capability for each candidate material in terms of $\mu mol/m^2$ and mg/m^2, as reported in Table 1. Under the selected standard conditions, an order of magnitude of difference is seen between weak and strong candidate materials, with carbon black and CoS at 1.3 $\mu mol/m^2$ and 2.6 $\mu mol/m^2$ respectively, compared to MnO_2 and V_2O_5 at 22.5 $\mu mol/m^2$ and 23.1 $\mu mol/m^2$ respectively.

It must be mentioned that while UV–vis is a useful technique for polysulfide adsorption capability analysis, extreme care is required throughout the procedure, and caution must be applied towards any quantitative data obtained. Lithium polysulfide species such as Li_2S_6 can undergo disproportionation reactions to form other species such as Li_2S_4 and Li_2S_8, adding complications to the analysis with Li_2S_6 no longer being the sole species present. More importantly, these polysulfide species are not stable in the ambient environment, any slight exposure to air or moisture will quickly result in significant color fading and nullify the validity of any UV–vis analysis. Samples need to be prepared with adequate sealing and contaminants-free solvents, and the Beer-Lambert law analysis should only be employed as an approximation of numerical values.

Inductively coupled plasma atomic emission spectroscopy (ICP-AES) is further performed on the supernatant solutions to provide a more accurate quantitative analysis. ICP-AES can detect the total concentration of lithium and sulfur atoms regardless of their chemical state, and therefore is much less susceptible to complications brought about by the instability of Li_2S_6 species. Fig. 2a shows the linear relationship between ICP-AES lithium intensity and Li_2S_6 concentration. A similar relationship is shown in Fig. 2b for sulfur. The only source of lithium introduced to the samples are from the 3 mM Li_2S_6 species, therefore based on the concentration of lithium atoms remaining in supernatant solution, it is possible to determine the amount of lithium adsorbed on the candidate materials. Fig. 2c depicts the calculated Li_2S_6 adsorption capability data for candidate materials based on ICP-AES analysis of lithium content. The results match reasonably well with previous UV–vis approximations and similarly demonstrate one order of magnitude of difference between weak and

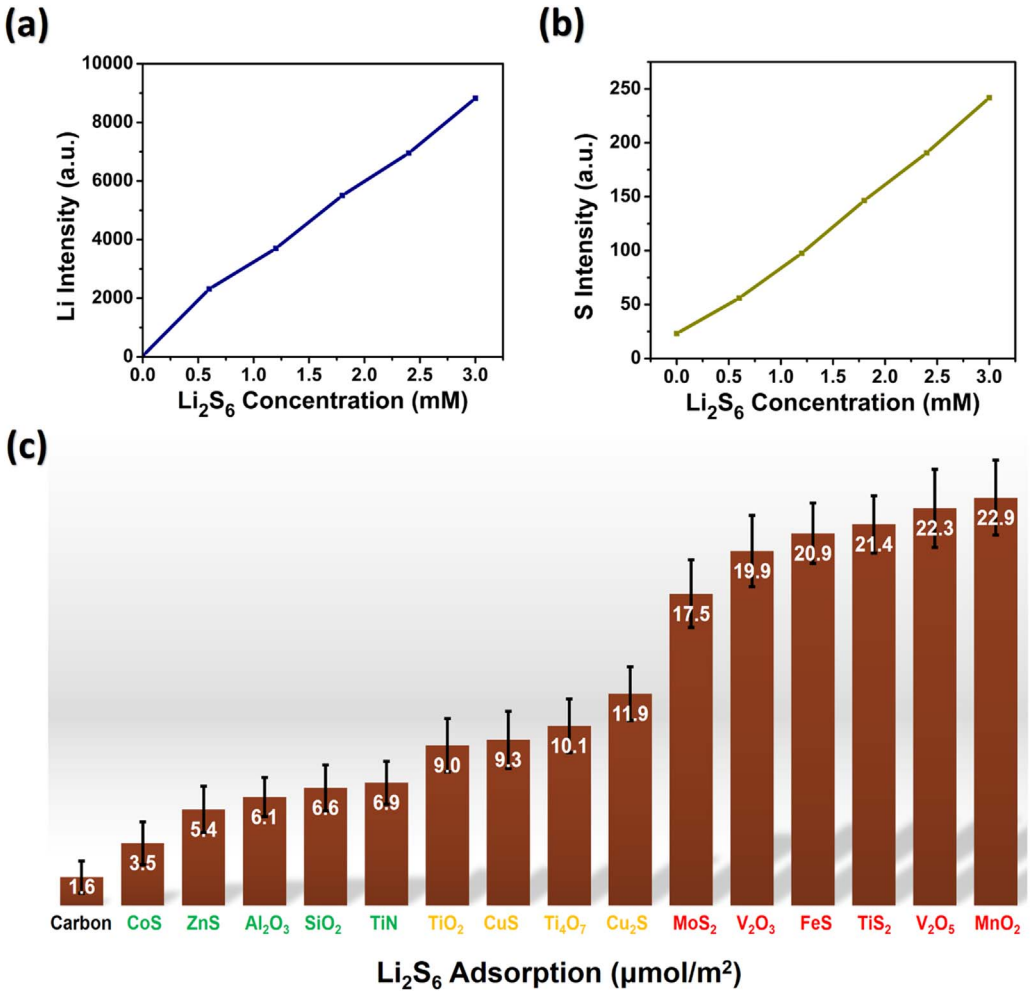

Fig. 2. Li_2S_6 polysulfide adsorption test. ICP-AES data of a) Li intensity and b) S intensity with varying Li_2S_6 concentrations without candidate materials, c) calculated adsorption by candidate materials in 3 mM Li_2S_6 solution.

strong candidate materials, with carbon black and CoS at 1.6 μmol/m^2 and 3.5 μmol/m^2 respectively, compared to MnO_2 and V_2O_5 at 22.9 μmol/m^2 and 22.3 μmol/m^2 respectively.

The assumption behind calculations in Fig. 2c is that the Li_2S_6 species stay intact and is the adsorbed species. This may not be true as the adsorbed species could be a mixture of different species, for example Li_2S_4 and Li_2S_2. Different candidate materials can have different preferences and mechanisms for the species adsorbed. Fig. 3a illustrates the sulfur to lithium content ratio of the supernatant solutions after Li_2S_6 adsorption tests. Based on the sulfur to lithium content, speculations can be made about the species present. A sulfur to lithium ratio of 3 corresponds with the original introduced species Li_2S_6, a ratio of 4 implies possible formation of the species Li_2S_8, while even higher ratios may suggest a mixture of S_8 and other lithium polysulfide species. Fig. 3b illustrates the calculated sulfur to lithium content ratio of the adsorbed species based on ICP-AES data. For carbon black, a S:Li ratio of 3 for both the remaining supernatant solution and the adsorbed species suggests that Li_2S_6 may be the adsorbed species. For Al_2O_3, SiO_2, TiN, TiO_2 and Ti_4O_7, a S:Li ratio of higher than 3 remaining in the supernatant solution suggests relatively more sulfur is left behind than lithium, and thus the adsorbed species should have a lower S:Li ratio than 3, this may correspond to a S:Li ratio of 2 for Li_2S_4, a ratio of 1 for Li_2S_2, and a ratio of 0.5 for Li_2S. For MnO_2, V_2O_5 and V_2O_3, S:Li ratios of much higher than 3 remain in the

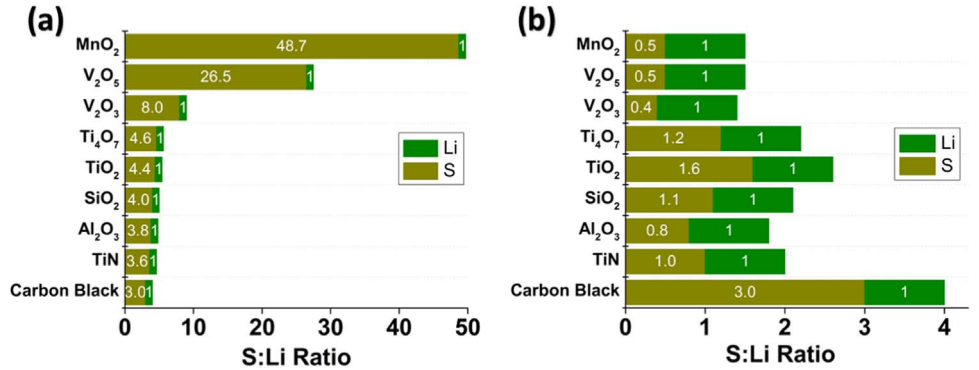

Fig. 3. ICP-AES data of S to Li atoms concentration ratio a) remaining in supernatant solutions and b) adsorbed onto candidate materials, after 3 mM Li_2S_6 adsorption test.

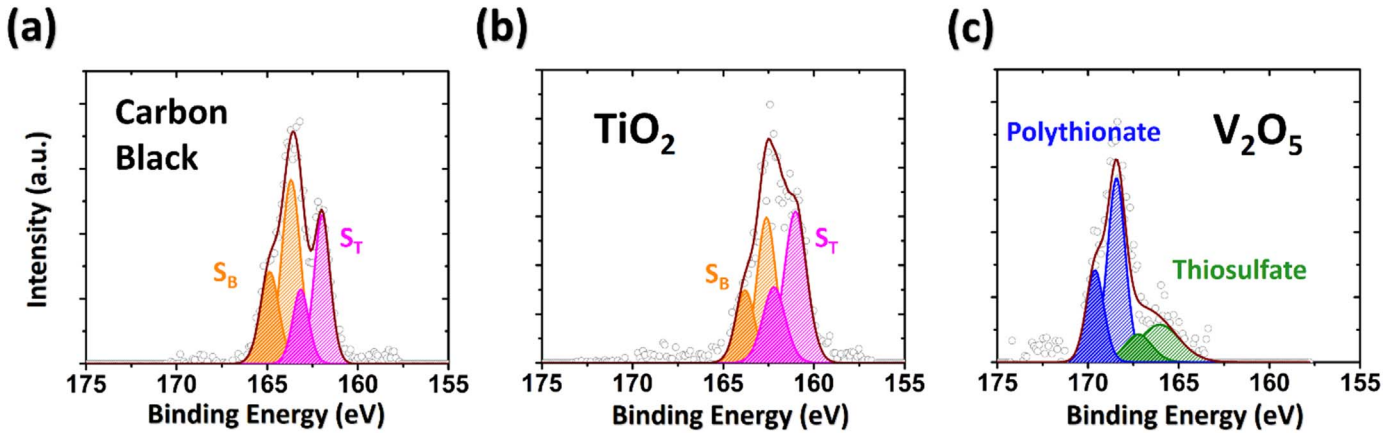

Fig. 4. XPS S 2p spectra of candidate materials surface after Li_2S_6 adsorption test for a) carbon black b) TiO_2 and c) V_2O_5.

supernatant solution, suggesting the adsorbed species would proportionally have higher lithium than the original Li_2S_6 species, and thus S:Li ratios much lower than 3. Therefore, it can be seen that the candidate materials can have different preferences for the proportional amount of sulfur and lithium adsorbed. In general, stronger candidate materials seem to adsorb relatively more lithium than sulfur, compared to weaker candidate materials. This is particularly evident in MnO_2, V_2O_5 and V_2O_3. The trend is also consistent in metal sulfides, with TiS_2, FeS and MoS_2 also exhibiting much higher preferences for lithium, however the S:Li ratios are not reported here because the metal sulfides themselves are a source of sulfur atoms and thus any powder particles that is suspended in supernatant solutions would severely undermine the validity of the S:Li ratio data for speculations of species adsorbed. It should also be noted that these ratios give the overall proportions of sulfur and lithium atoms, but do not provide information about the particular species present.

To further probe the interaction of candidate materials with polysulfides, X-ray photoelectron spectroscopy (XPS) studies are performed on the surface of candidate materials after adsorption tests. These give insight of the species adsorbed. Fig. 4 depicts a few representative cases while comprehensive data for candidate materials can be found in supporting information Figs. S1–S4. In the case of weak to moderate adsorption materials such as carbon black and TiO_2, polysulfides are the predominant observed species for sulfur 2p spectra, exhibiting "bridging" (S_B, 161.9 eV) sulfur and "terminal" (S_T, 163.7 eV) sulfur. This agrees with previous ICP-AES speculations that polysulfide species are adsorbed. For strong adsorption materials such as V_2O_5, polythionate (168.2 eV) and thiosulfate (167.2 eV) species are observed. This is in agreement with previous reports by the Nazar group [11,25]. Table 1 provides a summary of identified species present after adsorption tests. Battery cycling performance at 0.2 C and X-ray diffraction (XRD) data are also included in supporting information Figs. S5–S13 to provide additional details. XRD analysis displays an overall collection of facets without any bias towards particular surfaces, this in turn validates the generic nature of candidate materials.

4. Conclusion

In summary, we systematically investigated the polysulfide adsorption capabilities of 16 candidate materials. Our results indicate MnO_2 and V_2O_5 to be particularly strong materials and carbon black to be a particularly weak material for polysulfide adsorption. We made quantitative comparisons with normalized surface areas and observed an order of magnitude of difference across the candidate materials under equivalent conditions. The standard procedure we established is generic and can be further applied to more extensive lists of candidate materials. More importantly, this information can serve as a general guiding principle for the rational design of Li-S batteries when determining the suitable material and appropriate amount to employ for adequate polysulfide adsorption. Additional studies to understand the polysulfide adsorption mechanisms are paramount to addressing the polysulfide dissolution problem. These studies can provide much needed insight toward achieving practical Li-S batteries with high energy density and long cycle life [31–35].

Acknowledgment

Y.C. acknowledges support from the Assistant Secretary for Energy Efficiency and Renewable Energy, Office of Vehicle Technologies of the US Department of Energy, under the Battery Materials Research (BMR) program and Battery500 Consortium.

Appendix A. Supporting information

Supplementary data associated with this article can be found in the online version at doi:10.1016/j.ensm.2018.01.020.

References

[1] Z.W. Seh, Y. Sun, Q. Zhang, Y. Cui, Chem. Soc. Rev. 45 (20) (2016) 5605–5634.
[2] Y. Yang, G. Zheng, Y. Cui, Chem. Soc. Rev. 42 (7) (2013) 3018–3032.
[3] P. Adelhelm, P. Hartmann, C.L. Bender, M. Busche, C. Eufinger, J. Janek, J. Beilstein, Nanotechnology 6 (1) (2015) 1016–1055.
[4] A. Manthiram, S.H. Chung, C. Zu, Adv. Mater. 27 (12) (2015) 1980–2006.
[5] L.F. Nazar, M. Cuisinier, Q. Pang, MRS Bull. 39 (05) (2014) 436–442.
[6] H. Wang, Y. Yang, Y. Liang, J.T. Robinson, Y. Li, A. Jackson, Y. Cui, H. Dai, Nano Lett. 11 (7) (2011) 2644–2647.
[7] Y. Yang, G. Yu, J.J. Cha, H. Wu, M. Vosgueritchian, Y. Yao, Z. Bao, Y. Cui, ACS Nano 5 (11) (2011) 9187–9193.
[8] X. Ji, L.F. Nazar, J. Mater. Chem. 20 (44) (2010) 9821–9826.
[9] A. Manthiram, Y. Fu, S.H. Chung, C. Zu, Y.S. Su, Chem. Rev. 114 (23) (2014) 11751–11787.
[10] S. Evers, L.F. Nazar, Chem. Commun. 48 (9) (2012) 1233–1235.
[11] X. Liang, C.Y. Kwok, F. Lodi-Marzano, Q. Pang, M. Cuisinier, H. Huang, C.J. Hart, D. Houtarde, K. Kaup, H. Sommer, T. Breze-sinski, Adv. Energy Mater. 6 (2015) 1501636.
[12] X. Ji, S. Evers, R. Black, L.F. Nazar, Nat. Commun. 2 (2011) 325.
[13] M. Cuisinier, P.E. Cabelguen, S. Evers, G. He, M. Kolbeck, A. Garsuch, T. Bolin, M. Balasubramanian, L.F. Nazar, J. Phys. Chem. Lett. 4 (19) (2013) 3227–3232.
[14] S.H. Chung, A. Manthiram, Adv. Mater. 26 (9) (2014) 1360–1365.
[15] X. Ji, K.T. Lee, L.F. Nazar, Nat. Mater. 8 (6) (2009) 500–506.
[16] G. He, S. Evers, X. Liang, M. Cuisinier, A. Garsuch, L.F. Nazar, ACS Nano 7 (12) (2013) 10920–10930.
[17] N. Jayaprakash, J. Shen, S.S. Moganty, A. Corona, L.A. Archer, Angew. Chem. Int. Ed. 123 (26) (2011) 6026–6030.
[18] S. Evers, T. Yim, L.F. Nazar, J. Phys. Chem. C 116 (37) (2012) 19653–19658.
[19] Q. Pang, D. Kundu, M. Cuisinier, L.F. Nazar, Nat. Commun. 5 (2014) 4759.
[20] Y.J. Choi, B.S. Jung, D.J. Lee, J.H. Jeong, K.W. Kim, H.J. Ahn, K.K. Cho, H.B. Gu, Phys. Scr. T129 (2007) 62.
[21] X. Tao, J. Wang, C. Liu, H. Wang, H. Yao, G. Zheng, Z.W. Seh, Q. Cai, W. Li, G. Zhou, C. Zu, Nat. Commun. 7 (2016) 11203.
[22] Z.W. Seh, W. Li, J.J. Cha, G. Zheng, Y. Yang, M.T. McDowell, P.C. Hsu, Y. Cui, Nat. Commun. 4 (2013) 1331.

[23] X. Tao, J. Wang, Z. Ying, Q. Cai, G. Zheng, Y. Gan, H. Huang, Y. Xia, C. Liang, W. Zhang, Y. Cui, Nano Lett. 14 (9) (2014) 5288–5294.
[24] F. Lodi-Marzano, S. Leuthner, H. Sommer, T. Brezesinski, J. Janek, Energy Technol. 3 (8) (2015) 830–833.
[25] X. Liang, C. Hart, Q. Pang, A. Garsuch, T. Weiss, L.F. Nazar, Nat. Commun. 6 (2015) 5682.
[26] G. Zhou, H. Tian, Y. Jin, X. Tao, B. Liu, R. Zhang, Z.W. Seh, D. Zhuo, Y. Liu, J. Sun, J. Zhao, Proc. Natl. Acad. Sci. USA 114 (5) (2017) 840–845.
[27] Z. Cui, C. Zu, W. Zhou, A. Manthiram, J.B. Goodenough, Adv. Mater. 28 (32) (2016) 6926–6931.
[28] Q. Pang, D. Kundu, L.F. Nazar, Mater. Horiz. 3 (2) (2016) 130–136.
[29] Z.W. Seh, Q. Zhang, W. Li, G. Zheng, H. Yao, Y. Cui, Chem. Sci. 4 (9) (2013) 3673–3677.
[30] Q. Zhang, Y. Wang, Z.W. Seh, Z. Fu, R. Zhang, Y. Cui, Nano Lett. 15 (6) (2015) 3780–3786.
[31] D. Zheng, X. Zhang, J. Wang, D. Qu, X. Yang, D. Qu, J. Power Sources 301 (2016) 312–316.
[32] D. Zheng, D. Qu, X.Q. Yang, X. Yu, H.S. Lee, D. Qu, Adv. Energy Mater. 5 (16) (2015).
[33] D. Zheng, X. Zhang, C. Li, M.E. McKinnon, R.G. Sadok, D. Qu, X. Yu, H.S. Lee, X.Q. Yang, D. Qu, J. Electrochem. Soc. 162 (2015) A203–A206.
[34] T.Z. Hou, W.T. Xu, X. Chen, H.J. Peng, J.Q. Huang, Q. Zhang, Angew. Chem. Int. Ed. 56 (28) (2017) 8178–8182.
[35] X. Chen, H.J. Peng, R. Zhang, T.Z. Hou, J.Q. Huang, B. Li, Q. Zhang, ACS Energy Lett. 2 (4) (2017) 795–801.